

Integrated model for estimating phosphor signal and noise transfer characteristics on medical images: application to CdPO₃Cl:Mn phosphor screens

D. Cavouras¹ I. Kandarakis¹ G. S. Panayiotakis² C. D. Nomicos³

¹Department of Medical Instrumentation Technology, Technological Educational Institution of Athens, Athens, Greece

²Department of Medical Physics, Medical School, University of Patras, Patras, Greece

³Department of Electronics, Technological Educational Institution of Athens, Athens, Greece

Abstract—An integrated model describing the signal and noise transfer characteristics of the objective image quality and information content in phosphor-produced images is presented. In the context of this model, important imaging parameters, namely optical gain, modulation transfer function, noise transfer function, detective quantum efficiency and information capacity were experimentally evaluated using seven laboratory-prepared CdPO₃Cl:Mn test phosphor screens of varying coating thickness. This phosphor has been previously shown to exhibit high spectral compatibility properties with the films and optical sensors used in digital imaging systems. Experiments were performed using 50–120 kVp X-rays produced by a medical X-ray unit. Results showed that, for thick screens, optical gain attained peak values close to 200 optical photons per incident X-ray at 50 kVp. The noise transfer function was higher than the modulation transfer function. For the thin screen of 21 mg cm⁻², the modulation transfer function was 0.25 at 100 line pairs mm⁻¹, and the corresponding noise transfer function was 0.4. The detection quantum efficiency peak value was 0.22 at 50 kVp. These values are within acceptable performance limits, and, given the phosphor material's high spectral compatibility and medium temporal response, CdPO₃Cl:Mn could be considered for use in X-ray detectors of static radiography imaging.

Keywords—X-ray imaging, Phosphor screens, Modulation transfer function, Detective quantum efficiency, Information capacity

Med. Biol. Eng. Comput., 2002, 40, 273–277

1 Introduction

MEDICAL IMAGES are evaluated using physical parameters describing signal and noise transfer through imaging detectors and quantifying image quality and image information content (DAINTY and SHAW, 1974; KANAMORI and MATSUMOTO, 1984; SHAW and VAN METTER, 1984; ICRU, 1986; BUNCH *et al.*, 1987). In the case of images produced by phosphor-based detectors (radiographic cassettes, image intensifiers, flat panel detectors, computed tomography detectors), these parameters are related to the intrinsic physical processes of X-ray radiation absorption, X-ray conversion into light, and light transport to the output of the phosphor detector (LUDWIG, 1971; SWANK, 1973; SHAW and VAN METTER, 1984).

In the present study, an integrated model for the systematic estimation of phosphor material performance is presented. The model is based on the fundamental physical property of optical fluence emission and expresses signal, noise, image quality and image information content using the following parameters: detector optical gain (DOG), modulation transfer function (MTF), noise power spectrum (NPS) and noise transfer function (NTF), detective quantum efficiency (DQE) and information capacity (IC) (DAINTY and SHAW, 1974; EVANS, 1981; SHAW and VAN METTER, 1984; KANAMORI and MATSUMOTO, 1984; ICRU, 1986; BUNCH *et al.*, 1987; VAN METTER, 1992; KALIVAS *et al.*, 1999; KANDARAKIS *et al.*, 1999; KANDARAKIS and CAVOURAS, 2001a,b).

Results concerning some of the aforementioned image parameters, namely DOG, MTF, NTF, DQE and IC, were determined using a set of laboratory-prepared CdPO₃Cl:Mn phosphor screens. This phosphor has never been used in medical imaging applications. However, as has been previously demonstrated (KANDARAKIS *et al.*, 2001b), its emission spectrum exhibits high compatibility with the spectral sensitivity of the optical sensors, i.e. close to 0.9 with digital imaging amorphous silicon TFT sensors, and higher compatibility than rare earth phosphors with

Correspondence should be addressed to Prof. D. Cavouras;
email: cavouras@medisp.teiath.gr

Paper received 14 December 2001 and in final form 27 February 2002
MBEC online number: 20023667

© IFMBE: 2002

CCDs and film employed in digital and conventional imaging. Thus it could be considered for use in conventional and digital static imaging applications, given its medium decay time.

2 Materials and methods

2.1 Definitions

The output signal of a phosphor screen can be expressed in terms of the input signal and the gain transfer function, as follows:

$$\bar{\Phi}_\lambda(u, w) = \bar{\Phi}_X G_P(u, w) \quad (1)$$

where $\bar{\Phi}_\lambda$ denotes the optical fluence emitted by the phosphor screen, constituting the output signal. $\bar{\Phi}_X$ is the X-ray fluence incident on the phosphor or the input signal. G_P is the gain transfer function, characterising the signal transfer properties of the phosphor screen. The variables u and w represent the spatial frequency and the coating thickness of the phosphor screen, respectively. $\bar{\Phi}_\lambda$ and G_P are functions of the intrinsic physical processes of radiation absorption, conversion into light and light transport (SHAW and VAN METTER, 1984; KANDARAKIS and CAVOURAS, 2001a;b). (1) can be expressed in terms of the modulation transfer function $M_P(u, w)$ as follows:

$$\bar{\Phi}_\lambda(u, w) = \bar{\Phi}_X G_P(w) M_P(u, w) \quad (2)$$

where $G_P(w)$ is the zero-frequency gain transfer function or detector optical gain, expressing the number of emitted optical photons per incident X-ray photon and defined as follows:

$$G_P(w) = \frac{\bar{\Phi}_\lambda(0, w)}{\bar{\Phi}_X} \quad (3)$$

$M_P(u, w)$ in (2) is the modulation transfer function defined by the ratio (KANDARAKIS *et al.*, 1999)

$$M_P(u, w) = \frac{\bar{\Phi}_\lambda(u, w)}{\bar{\Phi}_\lambda(0, w)} \quad (4a)$$

The output noise can be expressed by the noise amplitude spectrum $A_P(u, w)$, the noise power (or Wiener) spectrum $W_P(u, w)$ (square of A_P) or the noise transfer function N_P (KANDARAKIS *et al.*, 1997; KALIVAS *et al.*, 1999), defined as

$$N_P(u, w) = \frac{W_P(u, w)}{W_P(0, w)} \quad (4b)$$

The zero-frequency noise power spectrum value $W_P(0, w)$ is equal to the variance of the output signal. The noise power spectrum $W_P(u, w)$ (and NTF) can be expressed in terms of $\bar{\Phi}_\lambda$, $M_P(u, w)$ and of intrinsic parameters related to the X-ray absorption and X-ray-to-light conversion processes (SHAW and VAN METTER, 1984; KANDARAKIS *et al.*, 1997; KALIVAS *et al.*, 1999).

Thus the output signal-to-noise ratio and the detective quantum efficiency (KANDARAKIS and CAVOURAS, 2001a;b) can be expressed as follows:

$$\begin{aligned} SNR_O(u, w) &= \frac{\bar{\Phi}_X G_P(u, w)}{A_P(u, w)} = \frac{\bar{\Phi}_X G_P(w) M_P(u, w)}{[W_P(u, w)]^{1/2}} \\ &= \frac{\bar{\Phi}_X G_P(w) M_P(u, w)}{[N_P(u, w) W_P(0, w)]^{1/2}} \end{aligned} \quad (5)$$

$$\begin{aligned} DQE(u, w) &= \frac{[SNR_O]^2}{[SNR_I]^2} = \frac{[\bar{\Phi}_X G_P(w) M_P(u, w)]^2}{W_P(u, w) SNR_I^2} \\ &= \frac{[\bar{\Phi}_X G_P(w) M_P(u, w)]^2}{N_P(u, w) W_P(0, w) SNR_I^2} \end{aligned} \quad (6)$$

The input signal-to-noise ratio SNR_I^2 has been previously considered to be equal to the incident X-ray fluence $\bar{\Phi}_X$ (SHAW and VAN METTER, 1984; KANDARAKIS *et al.*, 2001a). This follows from the Poisson statistical distribution, characterising the number of incident X-ray photons. Hence, DQE can be alternatively written as

$$\begin{aligned} DQE(u, w) &= \frac{[\bar{\Phi}_\lambda(w) M_P(u, w)]^2}{W_P(u, w) \bar{\Phi}_X} \\ &= \frac{[\bar{\Phi}_\lambda(w) M_P(u, w)]^2}{N_P(u, w) W_P(0, w) \bar{\Phi}_X} \end{aligned} \quad (7)$$

However, it must be pointed out that X-ray imaging detectors (SANDBORG and CARLSON, 1992; WILLIAMS *et al.*, 1999b) yield an output signal proportional to the total energy absorbed within the detector. Thus, the incident X-ray energy fluence $\bar{\Phi}_X E$, rather than X-ray photon fluence, should be used for input signal calculation. On the other hand, input noise has been expressed by the Poisson standard deviation of the X-ray photon fluence weighted by photon energy E (WILLIAMS *et al.*, 1999b), as follows:

$$SNR_{IN} = \frac{\int_0^{E_0} [d\bar{\Phi}_X(E)/dE] E dE}{[\int_0^{E_0} [d\bar{\Phi}_X(E)/dE] E^2 dE]^{1/2}} \quad (8)$$

where E is the energy of one X-ray quantum, and E_0 is the maximum energy of the spectrum of X-rays. $[d\bar{\Phi}_X(E)/dE]$ is the mean differential X-ray photon fluence spectral distribution (X-ray photon fluence per energy interval dE) averaged over the detector surface. This distribution has been previously described theoretically (STORM, 1972; TUCKER *et al.*, 1991) and calculated in terms of X-ray source characteristics.

Information capacity can provide an objective estimation of the image information content and describes overall image quality by a single index. Information capacity has been defined as $C_I = n_p \log_2 N_s$ (SHANNON, 1948; DAINTY and SHAW, 1974), i.e. in terms of the number of image elements (pixels) per unit of image area (n_p) and the number of distinguishable signal intensity levels (N_s) that can be registered in an image element. However, it has been previously found that IC can be expressed in terms of the output signal-to-noise ratio (DAINTY and SHAW, 1974; EVANS, 1981; KANAMORI and MATSUMOTO, 1984), as follows:

$$C_I(w) = \pi \int_0^\infty \log_2[1 + SNR_O^2(u, w)] u du \quad (9)$$

or

$$C_I(w) = \pi \int_0^\infty \log_2 \left[1 + \frac{[\bar{\Phi}_\lambda(w) M_P(u, w)]^2}{N_P(u, w) W_P(0, w)} \right] u du \quad (10)$$

and

$$C_I(w) = \pi \int_0^\infty \log_2[1 + \bar{\Phi}_X DQE(u, w)] u du \quad (11)$$

Information capacity is given in units of bits mm^{-2} . $\bar{\Phi}_X$ in (11) expresses SNR_{IN} , which, in case of polyenergetic beams, should normally be replaced by the expression in (8). As shown, if we use (1)–(11), DOG, MTF, NTF, DQE and IC can be expressed in terms of the same experimentally measurable quantities ($\bar{\Phi}_X$, $\bar{\Phi}_\lambda$) and, hence, they can be readily determined in laboratory.

2.2 Experimental part

DOG, MTF, NTF, DQE and IC were determined as follows:

Phosphor screens with various coating weights, from 21 to 160 mg cm^{-2} , were prepared in laboratory by sedimentation.

The phosphor material $\text{CdPO}_3\text{Cl:Mn}$ was in powder form, with a mean powder grain size of approximately $7\ \mu\text{m}$. Screens were irradiated by X-rays with tube voltages ranging from 50 to 120 kVp. The incident X-ray fluence Φ_X was determined by performing X-ray exposure measurements (GREENING, 1985). Optical fluence Φ_λ was measured during X-ray irradiation by a photomultiplier* coupled to an electrometer†.

Measurements were performed in reflection and transmission modes (irradiated and non-irradiated screen side, respectively) (KANDARAKIS *et al.*, 1999; KANDARAKIS and CAVOURAS, 2001a,b; KANDARAKIS *et al.*, 2001a). Optical fluence data were divided by the spectral matching factor 0.706 to be corrected for spectral compatibility mismatches with the photomultiplier's photocathode.

MTF was determined by the square wave response function (SWRF) (BARNES, 1979; ICRU, 1986; KANDARAKIS *et al.*, 1999), employing an MTF test pattern‡ and film**. It is of value to mention that $\text{CdPO}_3\text{Cl:Mn}$ exhibits higher spectral compatibility (matching factor) with this film (0.737) (KANDARAKIS *et al.*, 2001b) than currently used phosphors (0.52 for $\text{Gd}_2\text{O}_2\text{S:Tb}$), and it is adequately high for producing high-quality, low quantum noise images. The pattern–screen–film systems corresponding to each screen were irradiated with X-rays of 50–120 kVp. The films were then developed and digitised†† to obtain the digital pattern images (digital SWRF).

The MTFs were finally calculated from the digitised image optical density variations across directions vertical with respect to the images of the test pattern lines, employing the Coltman formula (ICRU, 1986). The latter gives MTF as a function of SWRF. MTF data obtained in this way were corrected by being divided by the MTF of the scanner and the MTF of the film, both measured in the same way (KANDARAKIS *et al.*, 1999; KANDARAKIS *et al.*, 2001a; CAVOURAS *et al.*, 1997).

The Wiener spectrum was determined by uniformly irradiating each phosphor screen placed in close contact with the film (BUNCH *et al.*, 1987). The same exposure geometry and X-ray tube voltages as in the case of MTF determination were employed, except that we did not use the MTF test pattern. After irradiation and film development, the film images were digitised. The noise power spectrum was determined by computing the Fourier transform of the optical density fluctuations (digital optical density values) (WILLIAMS *et al.*, 1999a; KALIVAS *et al.*, 1999; KANDARAKIS *et al.*, 2001a) obtained within an area of 1300×1300 pixels, each pixel corresponding to $21 \times 21\ \mu\text{m}^2$ on the radiographic film. Details of this measurement are given in previous studies (KALIVAS *et al.*, 1999; KANDARAKIS *et al.*, 2001a).

The input signal-to-noise ratio was determined using (8). The X-ray spectral distribution $[d\Phi_X/dE]$, obtained from data found in the literature (STORM, 1972; TUCKER *et al.*, 1991), was suitably modified to correspond to the X-ray tube characteristics used in the experiments.

3 Results and discussion

DOG was found to increase with phosphor thickness up to a certain value and to remain practically constant thereafter. At 80 kVp, in transmission mode measurements, the mean number of emitted optical photons per incident X-ray photon was found to vary between 125 and 165. Reflection mode measurements were 15–20% higher than the corresponding transmission mode

*EMI 9558 QB

†Cary 401

‡Type 53, Nuclear Associates

**Agfa Scopix LT2B

††Using a Microtec Scanmaker II SP, 1200×1200 dpi

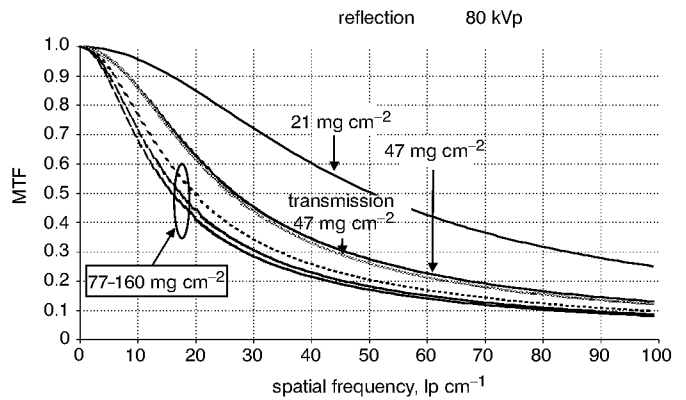


Fig. 1 Modulation transfer function determined at 80 kVp

measurements. Peak value was obtained for the $80\ \text{mg cm}^{-2}$ screen, whereas, for thicker screens, the number of optical photons was found to decrease slightly to 158 photons at $160\ \text{mg cm}^{-2}$ (transmission mode). DOG decreased continuously with X-ray tube voltage in the range between 60 and 120 kVp. For the $100\ \text{mg cm}^{-2}$ screen, the mean number of emitted photons was found to vary between 200 at 50 kVp and 140 at 120 kVp.

Fig. 1 shows MTF curves for various phosphor screens measured at 80 kVp in reflection mode. One curve obtained in transmission mode is also shown for comparison. The screen of $21\ \text{mg cm}^{-2}$ exhibited very high MTF values. The MTF of the $47\ \text{mg cm}^{-2}$ screen was found to be approximately 30–40% lower in the medium and high spatial frequency range, and the MTF curves of the screens thicker than $77\ \text{mg cm}^{-2}$ were found to be very close to each other. This degradation of MTF with screen thickness is explained by consideration of the effects of isotropic light emission and light scattering. These effects cause a spread of light photons during light transport, from the point of light creation to the screen output, which reduces the contrast and the resolution of the MTF test-pattern image. MTF data corresponding to other tube voltages are not shown, as their difference was not significant.

The shape of the curves describing NTF, shown in Fig. 2, is very similar to that of MTF. However NTF decreases more slowly than the corresponding MTF. At $100\ \text{lp mm}^{-1}$, the NTF of the $21\ \text{mg cm}^{-2}$ screen is equal to 0.4, whereas the corresponding MTF is 0.26. This difference, which is compatible with data published in previous studies (KANDARAKIS *et al.*, 1997), indicates that noise passes more efficiently than signals through a phosphor screen.

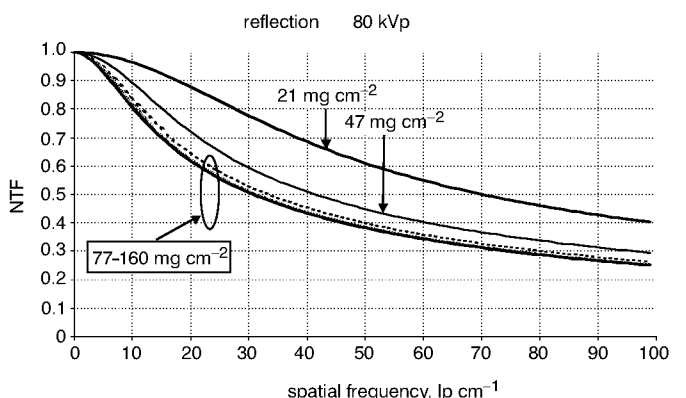


Fig. 2 Noise transfer function curves measured in reflection mode

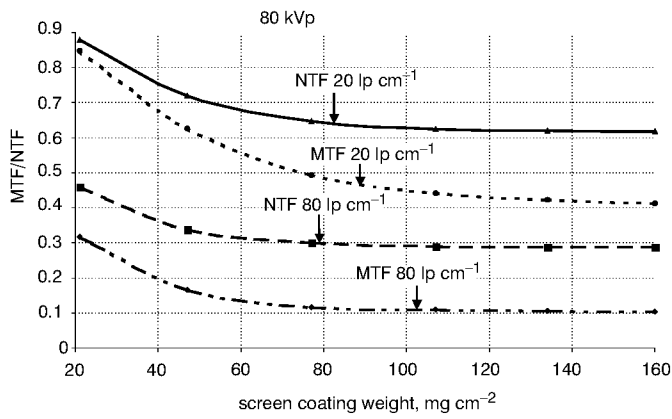


Fig. 3 Variation in MTF and NTF with screen thickness at 20 lp cm^{-1} and 80 lp cm^{-1} measure at 80 kVp

Fig. 3 depicts the variation of MTF and NTF with screen coating weight at two frequencies, namely at 20 lp cm^{-1} and 80 lp cm^{-1} . MTF curves in Fig. 3 aim to describe the deterioration in contrast and spatial resolution with increasing screen thickness. Contrast evaluates the ability to distinguish large objects from the surrounding background and can be indicated by MTF values at low frequencies (20 lp cm^{-1}). Spatial resolution shows the detail discrimination capability of an imaging system and can be expressed by MTF values at higher spatial frequencies (80 lp cm^{-1}) (CAVOURAS *et al.* 1998). NTF curves at 20 lp cm^{-1} and at 80 lp cm^{-1} describe the presence of noise in large object and small detail images, respectively. According to the results of Fig. 3, contrast, resolution and noise initially decrease rapidly with screen thickness, but the curves fall off very slowly for thick screens. It must be also mentioned that, in both cases, NTF is higher than MTF.

Fig. 4 displays the results concerning the detective quantum efficiency determined according to (7), employing values of the previously determined parameters Φ_λ , Φ_X , M_p , W_p . DQE curves were evaluated at 80 kVp and for various screen-coating thicknesses. DQE curves concerning transmission mode measurements are not shown, because their differences from the reflection DQE curves were not significant.

At the low-frequency range, the 107 , 134 and 160 mg cm^{-2} screens attained maximum DQE values, whereas the thinner 21 , 47 and 77 mg cm^{-2} screen curves showed lower DQE values. However, the 21 and 47 mg cm^{-2} thin screens decreased slowly with frequency, exhibiting slightly higher values than the thick ones in the high-frequency range. In the low spatial frequency range, DQE differences between screens are principally due to the effect of X-ray absorption, which is more significant in thick

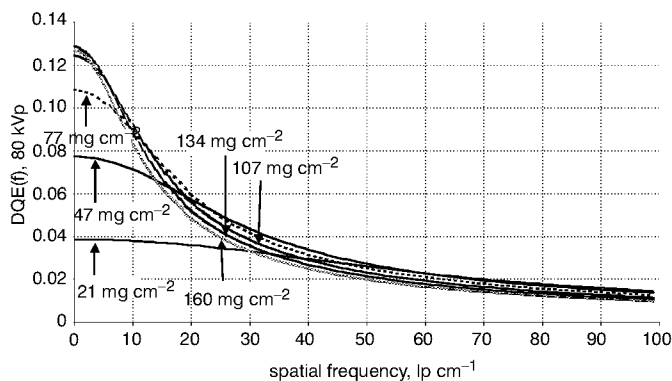


Fig. 4 Detective quantum efficiency determined at 80 kVp

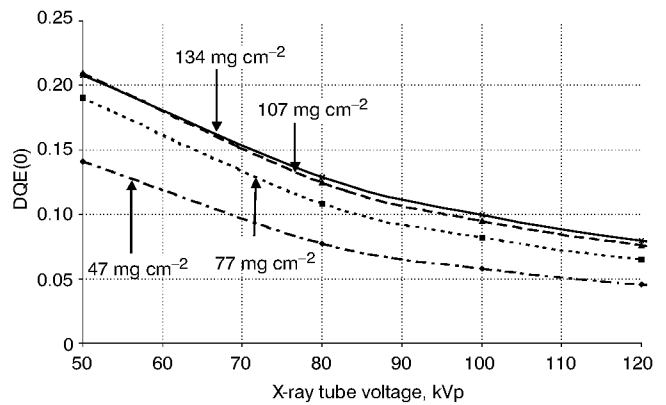


Fig. 5 Zero-frequency detective quantum efficiency as function of X-ray tube voltage

screens, causing a corresponding increase in emitted light flux and, hence, in DQE. At high spatial frequencies, thin screens maintain higher MTF values that compensate for the lower emitted light flux, thus resulting in slightly higher DQE values than those of thick screens.

Fig. 5 shows the variation in DQE with tube voltage. At zero frequency, it can be observed that DQE values decrease with increasing X-ray tube voltage. This may be owing to higher X-ray absorption at low X-ray energies, resulting in better Φ_λ values for a given level of incident X-ray fluence Φ_X . Similar to the frequency-dependent DQE (Fig. 4), for the same tube voltage, thick screens absorb larger fractions of incident X-rays, giving higher values of emitted light flux and, as a consequence, higher zero-frequency DQE values. Both frequency-dependent and zero-frequency DQE values found in this study are within or close to values found in previous studies concerning other phosphor materials (BEUTEL *et al.*, 1993; KANDARAKIS and CAVOURAS, 2001a;b).

Fig. 6 shows the information capacity, calculated according to (9) or (10), at 80 kVp , as a function of screen coating thickness. It can be observed that reflection mode data are slightly higher than transmission data, as was expected from the corresponding variation in MTF values. In both cases, however, information capacity shows a very slight variation with thickness, being approximately 20% higher for the 21 mg cm^{-2} screen with respect to the thickest screen. However, it must be noted that the information capacity of thin screens is mainly determined by the high MTF values, whereas the role of the emitted light fluence is more significant in the case of thick screens. IC values of this study were similar to values found in our previous studies on various phosphor materials (KANDARAKIS *et al.*, 1999).

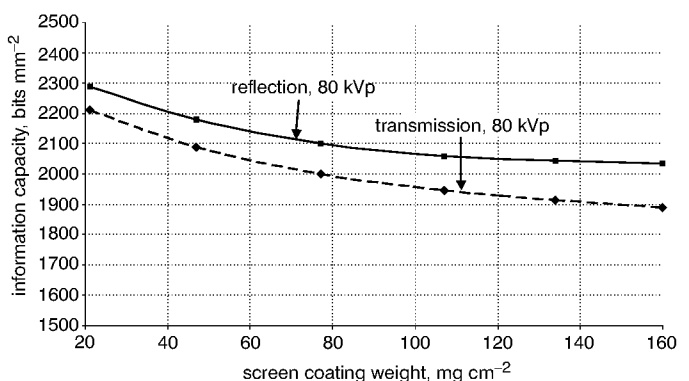


Fig. 6 Information capacity as function of screen coating thickness, determined at 80 kVp

However, it is difficult to make comparison with values found by other authors (KANAMORI and MATSUMOTO, 1984) in a very limited number of studies, as IC is very sensitive to X-ray exposure conditions (X-ray fluence, X-ray spectrum), as shown in (11).

4 Conclusions

The integrated model developed may be a useful tool for the evaluation of phosphor material imaging performance. Employing this model, the signal and noise transfer characteristics of CdPO₃Cl:Mn were estimated. DOG, MTF, NTF, DQE and IC values were found to be within acceptable performance limits, comparable with those published previously. Additionally, considering the high spectral compatibility properties of CdPO₃Cl:Mn with films and optical sensors used in digital imaging systems, together with its medium temporal response (LUMILUX, 1989), CdPO₃Cl:Mn could be considered for use in X-ray detectors of static radiography imaging.

Acknowledgments—This study is dedicated to the memory of Professor G. E. Giakoumakis, leading member of our team, whose work on phosphor materials has inspired us to continue.

References

BARNES, G. T. (1979): 'The use of bar pattern test objects in assessing the resolution of film/screen systems', in HAUS, A. G. (Ed.): 'The physics of medical imaging: recording systems, measurements and techniques' (American Association of Physicists in Medicine, New York, 1979), pp. 138–151

BEUTEL, J., MICKEWICH, D. J., ISSLER, S. L., and SHAW, R. (1983): 'The image quality characteristics of a novel ultra-high resolution film/screen system', *Phys. Med. Biol.*, **38**, pp. 1195–1206

BUNCH, P. C., HUFF, K. E., and VAN METTER, R. (1987): 'Analysis of the detective quantum-efficiency of a radiographic film-screen combination', *J. Opt. Soc. Am. A*, **4**, pp. 902–909

CAVOURAS, D., KANDARAKIS, I., PRASSOPOULOS, P., KANELLOPOULOS, E., NOMICOS, C. D., and PANAYIOTAKIS, G. S. (1998): 'Experimental evaluation of noise equivalent passband, information capacity, and informational efficiency of yttrium based europium activated phosphors', *Phys. Medica*, **14**, pp. 119–126

DAINTY, J. C., and SHAW, R. (1974): 'Image science' (Academic Press, London, 1974)

EVANS, A. L. (1981): 'The evaluation of medical images' (Adam Hilger, Bristol, 1981)

GREENING, J. R. (1985): 'Fundamentals of radiation dosimetry' (Medical Physics Handbooks, Institute of Physics, London, 1985)

ICRU (1986): 'Modulation transfer function of screen-film systems'. ICRU report 41

KALIVAS, N., KANDARAKIS, I., CAVOURAS, D., COSTARIDOU, L., NOMICOS, C. D., and PANAYIOTAKIS, G. (1999): 'Modeling quantum noise of phosphors used in medical X-ray image detectors', *Nucl. Instrum. Methods Phys. Res. A*, **430**, pp. 559–569

KANAMORI, H., and MATSUMOTO, M. (1984): 'The information spectrum as a measure of radiographic image quality and system performance', *Phys. Med. Biol.*, **29**, pp. 303–313

KANDARAKIS, I., CAVOURAS, D., PANAYIOTAKIS, G. S., and NOMICOS, C. D. (1997): 'Evaluating x-ray detectors for radiographic applications: A comparison of ZnSCdS:Ag with Gd₂O₂S:Tb and Y₂O₂S:Tb screens', *Phys. Med. Biol.*, **42**, pp. 1351–1373

KANDARAKIS, I., CAVOURAS, D., KANELLOPOULOS, E., NOMICOS, C. D., and PANAYIOTAKIS, G. S. (1999): 'A method for determining the information capacity of X-ray imaging scintillator detectors by means of luminescence and mtf measurements', *Med. Biol. Eng. Comput.*, **37**, pp. 25–30

KANDARAKIS, I., and CAVOURAS, D., (2001a): 'Experimental and theoretical assessment of the performance of Gd₂O₂S:Tb and

La₂O₂S:Tb phosphors and Gd₂O₂S:Tb–La₂O₂S:Tb mixtures for x-ray imaging', *Eur. Radiol.*, **11**, pp. 1083–1091

KANDARAKIS, I., and CAVOURAS, D. (2001b): 'Role of the activator in the performance of scintillators used in x-ray imaging', *Appl. Rad. Isot.*, **50**, pp. 821–831

KANDARAKIS, I., CAVOURAS, D., PANAYIOTAKIS, G. S., and NOMICOS, C. D. (2001a): 'Experimental investigation of the optical signal, gain, signal to noise ratio and information content characteristics of X-ray phosphor screens', *Appl. Phys. B*, **72**, pp. 877–883

KANDARAKIS, I., CAVOURAS, D., NOMICOS, C. D., and PANAYIOTAKIS, G. S. (2001b): 'Measurement of X-ray luminescence and spectral compatibility of CdPO₃Cl:Mn phosphor', *Radiat. Meas.*, **33**, pp. 217–224

LUDWIG, G. W. (1971): 'X-ray efficiency of powder phosphors', *J. Electrochem. Soc.*, **118**, pp. 1152–1159

LUMILUX (1989): 'Lumilux data book' (Riedel-deHaen, Seelze, Germany, 1989)

SANDBORG, M., and CARLSSON, G. A. (1992): 'Influence of x-ray spectrum, contrasting detail and detector on the signal to noise ratio and detective quantum efficiency in projection radiography', *Phys. Med. Biol.*, **33**, pp. 1245–1263

SHANNON, C. E. (1948): 'A mathematical theory of communication', *Bell. Syst. Tech. J.*, **27**, pp. 379–423

SHAW, R., and VAN METTER, R. (1984): 'An analysis of the fundamental limitations of screen-film systems for x-ray detection', *Proc. SPIE*, **454**, pp. 128–132

STORM, E. (1972): 'Calculated bremsstrahlung spectra from thick tungsten targets', *Phys. Rev. A*, **5**, pp. 2328–2338

SWANK, R. K. (1973): 'Calculation of modulation transfer function of x-ray fluorescent screens', *Appl. Opt.*, **12**, pp. 1865–1870

TUCKER, D. M., BARNES, G. T., and CHAKRABORTY, D. B. (1991): 'Semi-empirical model for generating tungsten target X-ray spectra', *Med. Phys.*, **18**, pp. 211–218

VAN METTER, R. (1992): 'Describing signal transfer-characteristics of asymmetrical radiographic screen-film systems', *Med. Phys.*, **19**, pp. 53–58

WILLIAMS, M. B., MANGIAFICO, P. A., and SIMONI, P. U. (1999a): 'Noise power spectra of images from digital mammography detectors', *Med. Phys.*, **26**, pp. 1279–1293

WILLIAMS, M. B., SIMONI, P. U., SMLOWITZ, L., STANTON, M., PHILLIPS, W., and STEWART, A. (1999b): 'Analysis of the detective quantum efficiency of a developmental detector for digital mammography', *Med. Phys.*, **26**, pp. 2273–2285

Authors' biographies

DIONISIS CAVOURAS holds a BSc in Electronic Engineering, and MSc and PhD degrees in Systems Science, from The City University, London, UK. He is Professor of Medical Imaging at TEI-Athens. His research interests include medical image processing, pattern recognition and scintillator materials evaluation.

IOANNIS KANDARAKIS holds a Physics degree from Patras University, Greece. He received his DEA and Doctorate degrees in Medical Radiation Physics from Paul Sabatier University of Toulouse, France. He is Professor of Ionizing Radiation at TEI-Athens, Greece. He is active in scintillator materials evaluation for use in imaging detectors and image quality.

GEORGE S. PANAYIOTAKIS holds a degree in Physics and a PhD in Medical Physics from Patras University. He is Associate Professor at the Department of Medical Physics of Patras University. His research interests include mammography, scintillator materials evaluation, medical informatics, teleradiology and image quality.

CONSTANTINE D. NOMICOS holds a degree in Physics, an MSc in Electronics and a PhD in Solid-State Physics, from Athens University. He is Professor of Microprocessors at TEI-Athens, Greece. His research interests include scintillator materials evaluation, semiconductor physics, and electromagnetic field variations prior to earthquakes.